Available online on 15.04.2026 at http://jddtonline.info

Journal of Drug Delivery and Therapeutics

Open Access to Pharmaceutical and Medical Research

Open Access Full Text Article

Research Article

2D QSAR of Novel hybrid motifs of 4-nitroimidazole-piperazinyl tagged 1,2,3-triazoles for Anti-cancer Activity against Breast Cancer cell line MCF-7

Pranay Raikwar [1], Arun Kumar Rai [2]*, Shabnam Yadav [1], Nitin Singh Rajput [1], Shivraj Pandey [1], Megha Mishra [1], Pradeep Kumar Singour [1]

[1] Department of Pharmaceutical Chemistry, VNS Group of Institutions- Faculty of Pharmacy, Neelbud, Bhopal (M.P.) 462044.

[2] Department of Pharmaceutical Chemistry, Corporate Institute of PharmacyPatel Nagar Raisen Road Bhopal, Madhya Pradesh, India (462022)

Article Info:

Article History:

Received 17 Jan 2026
Reviewed 25 Feb 2026
Accepted 18 March 2026
Published 15 April 2026

Cite this article as:

Raikwar P, Rai AK, Yadav S, Rajput NS, Pandey S, Mishra M, Singour PK, 2D QSAR of Novel hybrid motifs of 4-nitroimidazole-piperazinyl tagged 1,2,3-triazoles for Anti-cancer Activity against Breast Cancer cell line MCF-7, Journal of Drug Delivery and Therapeutics. 2026; 16(4):109-119 *DOI: http://dx.doi.org/10.22270/jddt.v16i4.7662*

For Correspondence:

Arun Kumar Arun, Assistant Professor, Department of Pharmaceutical Chemistry, Corporate Institute of Pharmacy, Patel Nagar Raisen Road Bhopal, Madhya Pradesh, India (462022)

Abstract

Objective: To develop and validate a two-dimensional quantitative structure–activity relationship (2D-QSAR) model for novel 4-nitroimidazole-piperazinyl tagged 1,2,3-triazole derivatives and to identify key physicochemical descriptors governing their anticancer activity against the human breast cancer cell line MCF-7.

Results and Discussion: Several statistically acceptable QSAR models were obtained; among them, Model 1, incorporating Molar Refractivity, partition coefficient, Henry's law constant, mass, and molecular weight, showed the most favorable balance of correlation and error ($r \approx 0.45$, $r^2 \approx 0.20$, standard deviation ≈ 0.50) with a single outlier. Descriptor analysis indicated that Molar Refractivity is positively correlated with MCF-7 inhibitory activity, suggesting that bulkier or more polarizable substituents enhance cytotoxic potency, while the partition coefficient term supports a beneficial role of less polar, more lipophilic groups. The results demonstrate that the thermodynamic and electronic nature of substituents strongly influences activity and that even a moderate-fit 2D-QSAR model can serve as a useful predictive tool for prioritizing new analogues.

Conclusion: The 2D-QSAR study established that MCF-7 cell inhibitory activity of 4-nitroimidazole-piperazinyl tagged 1,2,3-triazole derivatives is primarily governed by Molar Refractivity, lipophilicity-related parameters, and other thermodynamic–electronic descriptors of the substituents. The optimized Model 1 provides a rational basis for designing new hybrids with higher molecular refractivity and appropriately tuned hydrophobic and electronic profiles to achieve improved anticancer potency, and the proposed QSAR framework can be applied to further scaffold optimization against breast cancer targets.

Keywords: Quantitative Structure Activity Relationship (QSAR), Anti-Cancer,imidazole, ChemDraw, MCF-7 Cell.

INTRODUCTION:

Cancer is a perplexing and terrifying illness, or group of illnesses. For over 200 million years, multicellular organisms have suffered from cancer; evidence of cancer in contemporary humans' progenitors dates back more than a million years. In contrast to many environmental disorders, parasites, and infectious diseases, cancer is not largely brought on by an outside force. Human cells that have, in a sense, lost control and been recruited and partially changed into pathogenic organisms or the building blocks of tumors are its agents of destruction. In Explaining Cancer (2018), Anya Plutynski states "Cancer can be compared to a car breaking down, an infectious disease, a process of natural selection, a process of development, or even the expansion of an ecological community"[1,2].

One kind of cancer that manifests differently in women is breast cancer (BC)[3]. The United States reported 268,670 new cases of BC in 2018. Worldwide, BC is a prevalent malignancy that impacts women[4]. BC may be divided into three types based on molecular and histological evidence: BC expressing human epidermal receptor 2 (HER2+), BC expressing hormone receptors (estrogen receptor (ER+) or progesterone receptor (PR+)), and triple-negative breast cancer (TNBC).The BC molecular features should serve as the foundation for the therapeutic strategies. Furthermore, the TNBC was classified into six groups: immunomodulatory (IM), basal-like 1 (BL-1), basal-like 2 (BL-2), mesenchymal (M), mesenchymal stem cell-like (MSL), and luminal androgen receptor (LAR)[5]. It's unclear exactly how breast cancer begins[6,7]. The most common type of BC, BC expressing HR, accounts for 60–70% of BC occurrences in affluent nations and only affects premenopausal women. Consequently, the most popular therapeutic strategy is hormonotherapy[8].

In India, breast cancer has surpassed cervical cancer as the leading cause of cancer-related deaths among women. Researchers throughout the world are under

pressure to create new therapies more quickly due to the rising incidence of breast cancer and the emergence of drug resistance to current anticancer medications[9-11]. The structure-based drug designing technique, which has emerged as a potent tool to improve the drug discovery processes, can be used to meet this demand in lead identification and optimization[12]. Additionally, a number of researchers investigated the potential of plant compounds like resveratrol, isoflavones, and indoles against cancer.

The development of contemporary medications for the treatment of cancer is greatly aided by the use of natural plant products. In light of this, maslinic acid, a member of the class of triterpenes (oleananes), was the subject of a thorough structure-activity connection investigation[13]. It is one of the significant anticancer drugs for which no three-dimensional quantitative structure–activity relationship (3D-QSAR) analysis has yet been published in order to identify the major structural regulating areas and various active and inactive locations[14]. In order to identify the critical regulatory elements governing the toxicity and anticancer activity of maslinic acid, a 3D-QSAR research was conducted on this natural series. A common pharmacophore was created because there is currently no structural information available for maslinic acid in its target-bound state[15].

This creates a pharmacophore template that mimics the bioactive conformation by using the molecular field-based similarity technique for the conformational search. To gain a deeper understanding of the structure-activity relationship (SAR), activity-atlas models were also created[16]. The active compounds' positive and negative electrostatic areas were also made visible using 2D-QSAR. As a result, more potent and effective maslinic acid analogs were created. This 2D-QSAR method had a distinct effect and was a useful predictive tool, mostly in pharmaceutical design.Nevertheless, obtaining a high-quality 3D-QSAR is a difficult undertaking. This is because accurate alignments for every compound with the least amount of noise are required, as well as high-quality and trustworthy biological data[17,18].

Although the male adrenal cortex can manufacture estrogen, estrogen hormone is a steroid molecule that performs important modulatory roles in physiological processes, particularly in females[19,20]. The ovaries and placenta cells are the primary sources of estrogen, which is produced through the interaction and activation of the estrogen receptors ER α and ERβ, which belong to the nuclear receptor superfamily of transcription factors and have highly conserved DNA- and ligand-binding domains[21–24]. The female reproductive tract, breast, liver, bone, brain, skin, colon, and salivary gland are among the various tissues that contain estrogen receptors[25–27]. Consequently, ER α controls a number of intricate physiological functions in humans.

However, through estrogen signaling, ER contributes to the development of cancers. Tumor surface ER α protein has the ability to bind to estrogen (17b-estradiol, E2) and subsequently contribute to the development of cancers through estrogen signaling. Consequently, the hormone-responsive genes that support DNA synthesis and cell division are activated[19]. The reproductive system (endometriosis, breast, ovarian, and prostate cancer), bone, lung cancer, cardiovascular disease, gastrointestinal disease, urogenital tract disease, neurodegenerative disorders, and cutaneous melanoma are among the tumors where this promotes the growth and spread of cancer cells[24]. Compared to 10% in healthy tissues, ER α is overextended in 50–80% of breast cancer tissues. Consequently, it has been determined that estrogen has a major role in the development of ER α positive breast cancer, which accounts for approximately 70–80% of all cases of breast cancer[28-30]. As a selective estrogen receptor modulator (SERM), 4-hydroxytamoxifen (4-OHT) increases the growth rate of the human breast cancer cell line MCF-7 in response to estrogens and decreases it in response to antiestrogens[31]. demonstrates the function of ERs in the various cancer cell types employed in this investigation. While the involvement of ERβ is still debatable, it can be observed that Er α α has promising roles in the development of breast cancer.

Conversely, ER and ERβ have a major impact on prostate cancer, with ER α using tumor growth-promoting actions and ERβ using tumor growth-suppressive effects[24,36,37]. By lowering fibrosis and immune response, ERβ inhibits the development of liver cancer. The role of ER carcinoma cells in the liver when ER α α is still debatable and encourages hepatocellular proliferation cooperates with ERβ.

Among the most significant organic compounds that are commonly found in molecules of interest in medicinal chemistry are heterocyclic compounds[44] and heterocyclic scaffolds[45]. Additionally, heterocycles that include nitrogen are crucial to life science because they exhibit a variety of biological functions, including representative alkaloids and other nitrogen. Serotonin[46], thiamine, popularly known as vitamin B1[47], atropine[48], the infamous morphine[49], and the majority of vitamins, nucleic acid, enzymes, co-enzymes, hormones, and alkaloids all contain N-based heterocycles as scaffolds.

These facts reveal and highlight the critical importance of heterocycles in contemporary drug design and drug discovery. Nitrogen heterocyclic molecules have always been appealing candidates to synthetic organic chemists due to their various biological activities.

A well-known idea in drug design and research, molecular hybridization of heterocyclic motifs relies on the combination of pharmacophoric moieties of several bioactive compounds. When compared to the parent medications, they create a new hybrid system with better activities[50].

One of the most thoroughly researched substances in both the natural and synthetic worlds are those that contain nitroimidazole[51–53]. Because of its many biological and pharmacological characteristics, imidazoles have garnered a lot of attention recently[54,55]. In addition to their clinically demonstrated anticoagulant and antithrombotic properties, several triazoles have demonstrated antibacterial and

anticancer properties[56,57]. This technique may also produce molecules with altered selectivity profiles, distinct or multiple modes of action, and less undesirable side effects.

A number of structural modification techniques have been used to rationally plan new synthetic prototypes with the goal of creating new compounds with optimized pharmacodynamic and pharmacokinetic properties. These techniques include investigating the fragments of bioactive substances (Fragment-Based Drug Design)[58], active metabolites of drugs[59], bioisosterism[60], selective optimization of drug side effects[61], and drug latentiation.

Because of their broad pharmacological profiles, which include antibacterial[64,65] and anticancer [66,67] properties, and their easy synthesis using click chemistry[62,63], 1,2,3-triazoles have a significant position in drug discovery. Potential structural characteristics of bioactive triazoles include their excellent selectivity, stability against metabolic degradation, and hydrogen bonding capacity, which may be advantageous when binding biomolecular targets[68]. It has been shown that various kinds of chemical bridges at the C-4 of the 1,2,3-triazole core remove planarity, which may improve drug-ability and make it easier for molecules to attach to potential receptors by induced fit.

Our team has been synthesizing several derivatives of novel 5-substituted piperazinyl-4-nitroimidazole derivatives and assessing their anti-HIV efficacy for the past fifteen years[69-71]. Because they circulate freely throughout the body and are irreversibly bound by nucleophilic covalent binding to proteins in low oxygen settings, nitroimidazoles are a popular class of compounds that have been thoroughly explored as molecular probes[72]. 4-Derivatives of nitroimidazoles have been investigated as radiopharmaceuticals for tumor hypoxia probe, therapeutic therapy, antifertility potential, and anti-tubercular profile[73,74]. The synthesis of the highly effective hybridization system that our group reported has been the subject of other investigations[75].

MATERIAL AND METHODS:

The Novel hybrid motifs of 4-nitroimidazole-piperazinyl tagged 1,2,3-triazoles derivatives chemicals produced by were the materials employed in this investigation. In Table 1, the dependent variable was the Inhibition Concentration (IC50)[76].

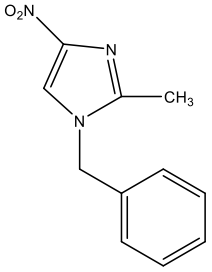

2

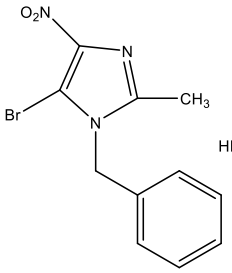

3

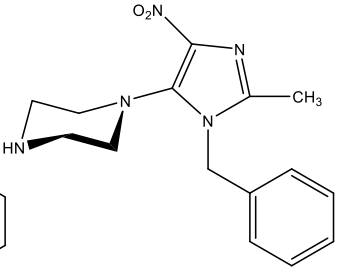

4

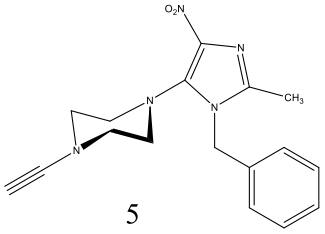

5

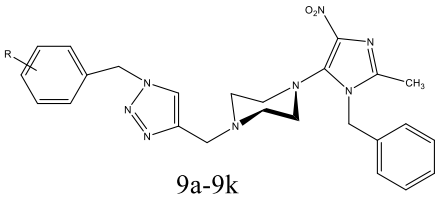

9a-9k

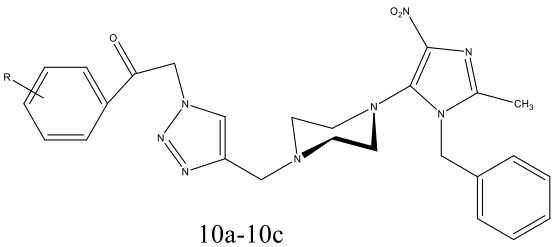

10a-10c

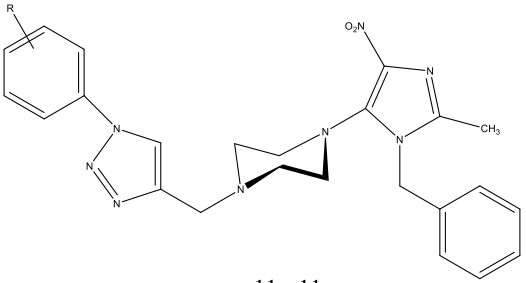

11a-11n

Table 1: Structure and biological activity of 4-nitroimidazole-piperazinyl tagged 1,2,3-triazoles

S. No.	Compounds	Substitution R	MCF-7 Cell Actual IC50 (µM)	Biological Activity
1.	COMPOUND 2	-	0.068	7.167491087
2.	COMPOUND 3	-	4.2	5.37675071
3.*	COMPOUND 4	-	0.085	7.070581074
4.	COMPOUND 5	--	0.084	7.075720714
5.	COMPOUND 9a	H	0.055	7.259637311
6.	COMPOUND 9b	p-Br	0.079	7.102372909
7.	COMPOUND 9c	p-F	0.024	7.619788758
8.	COMPOUND 9d	m-NO_2	0.04	7.397940009
9.	COMPOUND 9e	m-Me	0.079	7.102372909
10.	COMPOUND 9f	m—Br	0.053	7.27572413
11.	COMPOUND 9g	m-F	0.002	8.698970004
12.	COMPOUND 9h	o-NO_2	0.048	7.318758763
13.*	COMPOUND 9i	o-Br	0.106	6.974694135
14.	COMPOUND 9j	o-F	0.151	6.821023053
15.	COMPOUND 9k	p-Me	0.005	8.301029996
16.	COMPOUND 10a	H	0.112	6.950781977
17.	COMPOUND 10b	p-Br	0.372	6.42945706
18.	COMPOUND 10c	m-OME	0.585	6.232844134
19.	COMPOUND 11a	p-Br	2.12	5.673664139
20.	COMPOUND 11b	o-SMe	0.136	6.866461092
21.*	COMPOUND 11c	o-OEt	0.399	6.399027104
22.	COMPOUND 11d	H	0.312	6.879426069
23.	COMPOUND 11e	p-Me	0.219	6.659555885
24.	COMPOUND 11f	p-Ome	0.251	6.600326279
25.	COMPOUND 11g	o-Me	0.183	6.73754891
26.	COMPOUND 11h	o-Et	0.088	7.055517328
27.*	COMPOUND 11i	o-NO_2	0.185	6.732828272
28.	COMPOUND 11j	p-Cl	0.279	6.554395797
29.	COMPOUND 11k	P-NO_2	0.671	6.17327748
30.	COMPOUND 11l	m-OMe	0.198	6.70333481
31.	COMPOUND 11m	m-Me	0.161	6.793174124
32.	COMPOUND 11n	m-Cl	0.155	6.809668302
33.	COMPOUND 11o	Tetralin	0.131	6.882728704
34.	COMPOUND 11p	Benzdioxole	0.052	7.283996656
35.	COMPOUND 11q	Naphthalene	0.27	6.568636236

* **test set compounds**

Instrumentation:

An Asus laptop with an Intel® Core i5 processor, 8GB of RAM, and a 500GB SDD was utilized in this study. The package Chemoffice application Version 16.0 for Windows was used to calculate all of the compounds' physiochemical parameters (Table 1), and the semi-empirical Chem3D was used to finish geometry optimization. The statistical application Valstat version 16 for Windows was then used for analysis.

Data Set:

The physicochemical properties of novel hybrid motifs of 4-nitroimidazole-piperazinyl tagged 1,2,3-triazole derivatives were linked to their inhibitory action using QSAR analysis. The data series were taken from a study released by ***Sadeekah O.W. Saber et. al.,* 2023** There are 35 in the selected series. The structure and diversity of activities in both sets are thereby maintained for the purpose of creating QSAR models. The biological activities were expressed using the inhibitory concentration (IC50) in micromolar concentrations. For correlational purposes, the indicated IC50 values were first converted to their molar units and then to the free energy-related negative logarithmic state, or Log (1/IC50) or pIC50.

Descriptors calculation

Five steps are involved in the development of the QSAR model. The first step consists of determining the series of pyrazole-benzimidazole compounds to be studied and the IC50 value found in the lab experiment. The second stage is to select a set of descriptors that are likely related to the biological activity of interest in order to optimize for the most stable skeleton structure of the series of pyrazole-benzimidazole compounds. The next step is to compute descriptors using the optimized structure. In the fourth step, a mathematical equation model representing the relationship between the biological activity and the chosen descriptors is created using statistical analysis with VALSTAT Software for Windows. Validating the QSAR models is the final stage.

All of the pyrazole-benzimidazole derivative structures were displayed using Chem Draw 16.0. The molecular mechanics (MM2) technique was used to look for lower energy conformations in each molecule. Molecular orbital property accompanying name (MOPAC) was used to reoptimize the compounds with the lowest energy. To avoid the compounds' local stable conformations, the geometry of each molecule was optimized utilizing a range of starting points. When determining the molecular descriptors, the conformation with the lowest energy was considered[77]. The QSAR study's thermodynamic, electronic, steric, and molecular descriptors were computed using ChemOffice 2001 displayed in Table 2.

Table 2: Descriptors for training and test set compounds of series

S.NO	Henry's Law Constant	Mol Refractivity	Exact Mass	Mass	Mol Weight	Partition Coefficient	LogP	LogS	PKa
1	4.149	5.957299709	217.0851266	217.228	217.228	1.651100039	2.60282	-3.36199	0
2	4.149	6.73429966	294.9956392	296.124	296.124	2.326448202	3.39452	-4.1582	0
3	4.149	9.013700485	317.185175	317.393	317.393	3.054520607	3.5992	-4.48971	9.03019
4	4.149	10.20230103	355.2008251	355.442	355.442	4.067719936	4.12525	-4.82478	7.65804
5	4.149	13.97099972	488.2648223	488.596	488.596	4.600320339	5.16512	-7.05665	7.54281
6	4.149	14.74800014	566.1753349	567.492	567.492	5.463320732	5.96058	-7.8762	7.54152
7	4.149	13.98649979	506.2554005	506.5864032	506.5864032	4.743320465	5.32637	-7.28205	7.54332
8	4.149	14.5824995	533.2499005	533.593	533.593	4.343319893	5.05945	-7.4615	7.53104
9	4.149	14.43480015	502.2804724	502.623	502.623	5.099320412	5.60228	-7.41656	7.54227
10	4.149	14.74800014	566.1753349	567.492	567.492	5.463320732	5.96058	-7.87423	7.53708
11	4.149	13.98649979	506.2554005	506.5864032	506.5864032	4.743320465	5.32637	-7.27844	7.53794
12	4.149	14.5824995	533.2499005	533.593	533.593	4.263319969	5.05945	-7.45935	7.47959
13	4.149	14.74800014	566.1753349	567.492	567.492	5.463320732	5.96058	-7.87469	7.50477
14	4.149	13.98649979	506.2554005	506.5864032	506.5864032	4.743320465	5.32637	-7.27989	7.48475
15	4.149	14.43480015	502.2804724	502.623	502.623	5.099320412	5.60228	-7.41794	7.54303
16	4.149	14.47049999	516.2597369	516.606	516.606	4.217520237	4.78923	-6.98457	7.41852
17	4.149	15.24749947	594.1702495	595.502	595.502	5.156120777	5.58469	-7.79803	7.41912
18	4.149	15.08740044	546.2703016	546.632	546.632	4.437420845	4.69171	-6.99903	7.41652
19	4.149	14.28419971	552.1596848	553.465	553.465	6.086218357	5.82578	-7.77518	7.47903

20	4.149	14.77729988	520.236893	520.656	520.656	5.692176342	5.79707	-7.77285	7.47775
21	4.149	15.24109936	534.2525431	534.683	534.683	6.221176147	6.13665	-8.04249	7.47594
22	4.149	13.50719929	474.2491722	474.569	474.569	5.051320076	5.03032	-6.9576	7.48437
23	4.149	13.97099972	488.2648223	488.596	488.596	5.550319195	5.46748	-7.30925	7.48664
24	4.149	14.12409973	504.2597369	504.595	504.595	5.279327393	4.9328	-7.00997	7.50118
25	4.149	13.97099972	488.2648223	488.596	488.596	5.550319195	5.2541	-7.15653	7.49842
26	4.149	14.43480015	502.2804724	502.623	502.623	6.079319954	5.72377	-7.51987	7.4889
27	4.149	14.11869907	519.2342505	519.566	519.566	5.162673473	4.92465	-7.33855	7.21096
28	4.149	13.99859905	508.2101999	509.011	509.011	5.936218262	5.6523	-7.65374	7.47595
29	4.149	14.11869907	519.2342505	519.566	519.566	5.162673473	4.92465	-7.35822	7.44963
30	4.149	14.12409973	504.2597369	504.595	504.595	5.279327393	4.9328	-7.0175	7.43033
31	4.149	13.97099972	488.2648223	488.596	488.596	5.550319195	5.46748	-7.31969	7.47759
32	4.149	13.99859905	508.2101999	509.011	509.011	5.936218262	5.6523	-7.65175	7.43716
33	4.149	15.18500042	528.2961224	528.661	528.661	6.623319149	6.26172	-8.19125	7.47969
34	4.149	14.09979916	518.2390015	518.578	518.578	5.262735844	4.78137	-7.11108	7.44531
35	4.149	15.19519901	524.2648223	524.629	524.629	6.225319386	6.29714	-8.35474	7.46446

Statistical analysis:

The estimated descriptors for each enzyme inhibitory activity were gathered using a data matrix (D) with a dimension of (n × m). The number of molecules in each data set and the number of computed descriptors for each molecule are denoted by the numbers n and m, respectively. Initially, the descriptors were checked for constant or almost constant values, and those that were discovered were removed from the initial data matrix. Next, the relationship between the activity data and the descriptors was determined. To do the correlation study and identify the primary factors impacting the activity, the statistical tool VALSTAT was utilized.

Model development and validation:

QSAR models yielded multiple linear regression (MLR) analysis. The stepwise selection of variables, which combines forward selection and backward elimination techniques, was used to pick the most relevant subset of descriptors. Regression analysis was performed with the VALSTAT program.

External validation was used to validate the QSAR model. This method is used to calculate the activity of each compound in the test set. The calculated and observed activities were used to construct the cross-validation coefficient q2. One way to gauge a model's stability and predictive accuracy is to look at its cross-validation coefficient, or q2. The square of the cross-validation coefficient (q2) should be at least 0.5 for a reliable model.

RESULT AND DISCUSSION:

Molar Refractivity, Mass, Partition Coefficient, LogP, LogS, Polar Surface Area, Sum of Degree, Sum of Val. Degree, and Wiener Index are among the descriptors employed in this investigation. The descriptors were obtained from the structural characteristics of each compound after the geometry optimization process. The descriptors of the series of pyrazole-benzimidazole compounds were obtained using the semi-empirical PM3 technique. This method can be used to analyze a variety of pyrazole-benzimidazole derivatives because they are organic compounds composed of the atoms C, H, and N. Regression analysis was used in the statistical study to identify the QSAR models and their statistical properties.

Multiple linear regressions and other statistical analysis were performed on every molecule in the training set. Descriptors were selected for the model based on their correlation coefficient; those with an interred correlation coefficient of less than 0.6 were taken into account. Numerous models were generated by multiple linear regression (MLR) analysis. The model's predictive power was evaluated using a variety of statistical measures, such as the correlation coefficient, regression coefficient (r2), Fischer statistical value (F), and standard error. All of these statistical features were computed, according to the VALSTAT.

The first regression analysis was performed on each training molecule, resulting in a regression model. The best QSAR model has a large F, low p-value, r2 and q2 values near 1, and P<0.001. The best QSAR model created using the multiple linear regression (MLR) technique is represented by the following equation:

optimized model no. 1 results are.....

BA= [6.33613(±0.565209)] +Exact [-0.348746(± 0.185605)] +Mass [-0.169603(± 0.173082)] +Mol [0.149827(±0.0646368)]

n=34,r=0.451694,r^2=0.204027,r^2adj=0.12443,variance= 0.245301,std=0.495279,QF=0.911999, PE=0.0910055, F=2.56325, FIT=0.180592, LOF=11.6695, AIC=0.29865standard Fmax value at 95% confidence=5.58871

Henry's law Constant, Partition Coefficient, and Mass, Molecular weight, descriptors with r^2 = 0.204027 and std = 0.495279 were used for developing Model 1. Std was higher and r^2 was lower. Thus, we created Model 2 and 3 by substituting the Mass descriptor for the logP descriptor, and we discovered Model 2 Value a r2 value of 0.192457 and a standard deviation of 0.572264. and Model 3 value is r2 value of 0.17021 and a standard deviation of0.580094.

optimizedmodel no. 2 results are.....

BA= [6.4112(±0.632438)] +Law [0.0885432(± 0.0949709)] +Exact [-0.347976(± 0.172289)] +Mol [0.144589(±0.0840339)]

n=35, r=0.438699, r^2=0.192457, r^2adj=0.114308, variance=0.327487, std=0.572264, QF=0.766603, PE=0.0909998, F=2.46269, FIT=0.16791, LOF=15.8626, AIC=0.411999standard Fmax value at 95% confidence=5.53414

optimizedmodel no. 3 results are.....

BA=[6.73489(±0.634665)] +Constant[0.000266736(±0.00219479)] +Exact [-0.248804(±0.16037)] +Mol [0.180689(±0.0785019)]

n=35, r=0.412565, r^2=0.17021, r^2adj=0.0899073, variance=0.336509, std=0.580094, QF=0.711203, PE=0.0935068, F=2.11961, FIT=0.144519, LOF=16.2996, AIC=0.42335standard Fmax value at 95% confidence=5.53414

We looked into creating several models utilizing different descriptors, and we found that Models 1, 2, and 3 had the descriptors Molar Refractivity along with Partition Coefficient, Henary law constant, Mass, and Exact mass. We found that model 1 is better than the other two models, with a r2 value of 0.204027, a standard deviation of 0.495279, and one outlier. MDB and MCF-7 inhibitor activity are positively correlated. The positive correlation of MR indicates that higher molecular weight or bulky group compounds are essential for enhanced MCF-7 cell inhibitory action. An electrophilic group would increase activity, according to the Molar Refractivity negative correlation.Furthermore, a correlation was found in the Partition Coefficient, indicating that less polar groups are more active. Table-3 and Figure-1 show the predicted pIC50 and biological activity values of the training and test sets of series using model-1. Figure-2 show the Residual value (RV= pIC50 – Actual Biological Activity).

Table 3: The Actual and predicted pIC50 values of the training set of series by using model-1

S.No	Compound No.	Predicted pIC50	Actual Biological Activity	Residual Value
1.	COMPOUND 2	5.52393	7.167491087	-1.64356
2.	COMPOUND 3	6.99796	5.37675071	1.621209
3.	COMPOUND 4	8.19896	7.070581074	1.128379
4.	COMPOUND 5	6.9808	7.075720714	-0.09492
5.	COMPOUND 9a	7.1358	7.259637311	-0.12384
6.	COMPOUND 9b	6.89882	7.102372909	-0.20355
7.	COMPOUND 9c	7.06426	7.619788758	-0.55553
8.	COMPOUND 9d	7.26196	7.397940009	-0.13598
9.	COMPOUND 9e	7.00167	7.102372909	-0.1007
10.	COMPOUND 9f	6.89148	7.27572413	-0.38424
11.	COMPOUND 9g	7.0117	8.698970004	-1.68727
12.	COMPOUND 9h	7.29712	7.318758763	-0.02164
13.	COMPOUND 9i	6.89818	6.974694135	-0.07651
14.	COMPOUND 9j	7.09358	6.821023053	0.272557
15.	COMPOUND 9k	6.95579	8.301029996	-1.34524
16.	COMPOUND 10a	7.35716	6.950781977	0.406378
17.	COMPOUND 10b	7.08861	6.42945706	0.659153
18.	COMPOUND 10c	7.4807	6.232844134	1.247856
19.	COMPOUND 11a	6.73711	5.673664139	1.063446
20.	COMPOUND 11b	6.81799	6.866461092	-0.04847
21.	COMPOUND 11c	6.702	6.399027104	0.302973

22.	COMPOUND 11d	6.93344	6.879426069	0.054014
23.	COMPOUND 11e	6.80588	6.659555885	0.146324
24.	COMPOUND 11f	6.91907	6.600326279	0.318744
25.	COMPOUND 11g	6.80403	6.73754891	0.066481
26.	COMPOUND 11h	6.62007	7.055517328	-0.43545
27.	COMPOUND 11i	6.91297	6.732828272	0.180142
28.	COMPOUND 11j	6.6763	6.554395797	0.121904
29.	COMPOUND 11k	6.96582	6.17327748	0.792543
30.	COMPOUND 11l	6.90521	6.70333481	0.201875
31.	COMPOUND 11m	6.79827	6.793174124	0.005096
32.	COMPOUND 11n	6.64654	6.809668302	-0.16313
33.	COMPOUND 11o	6.47422	6.882728704	-0.40851
34.	COMPOUND 11p	6.89301	7.283996656	-0.39099
35.	COMPOUND 11q	6.67894	6.568636236	0.110304

Compound 11 was outlier.

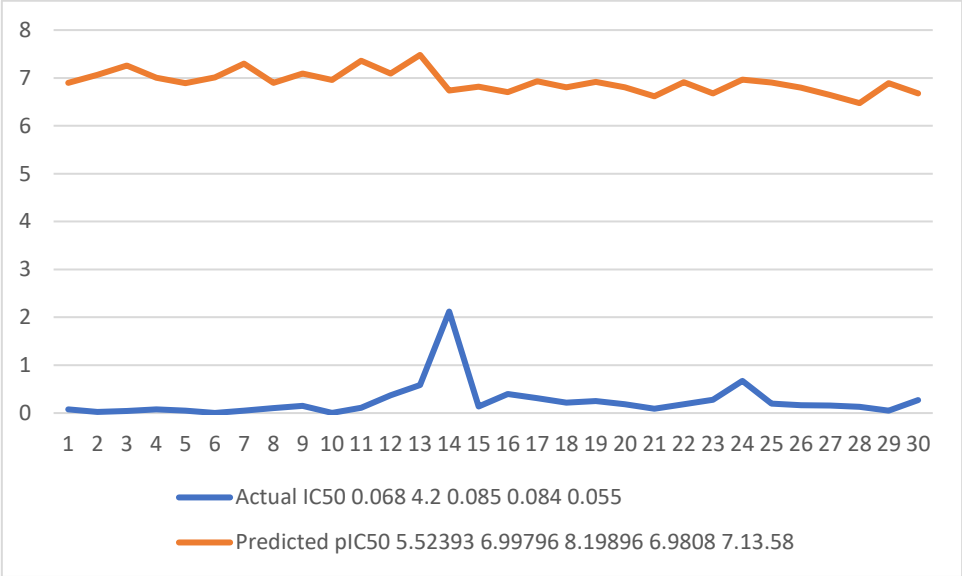

Figure 1: Corelation between Experimental IC50 value and Predicted pIC50 value.

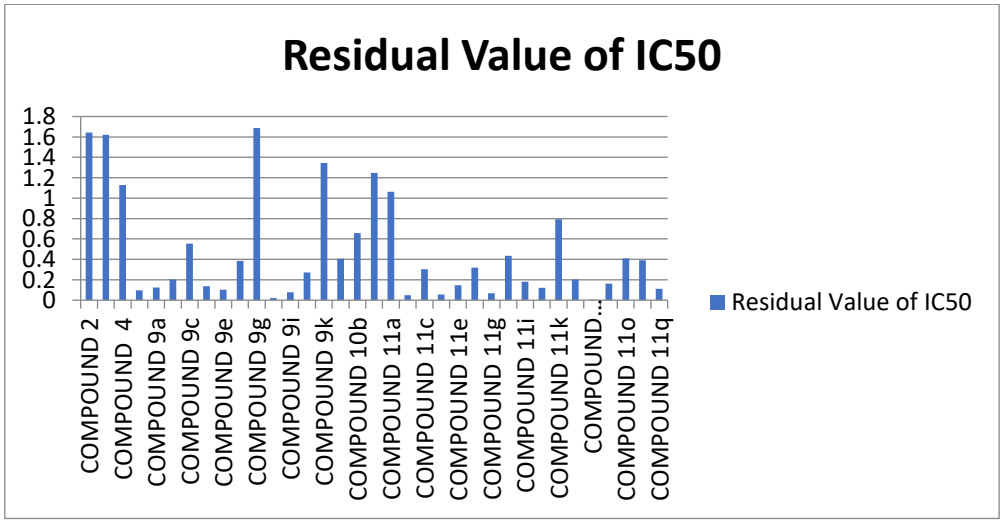

Figure 2: Graph of Residul value

CONCLUSION

For the MCF-7 cell inhibitory action of 4-nitroimidazole-piperazinyl tagged 1,2,3-triazoles compounds, we created a QSAR model. It is possible to determine that the MCF-7 inhibitory activity of 4-nitroimidazole-piperazinyl tagged 1,2,3-triazoles derivatives is significantly influenced by the thermodynamic and electrical nature of the substituents. According to the proposed QSAR model, the maximum Molar Refractivity, Partition coefficient, Henary law constant, and molecular weight should be taken into consideration while designing novel compounds for their potential MCF-7 inhibitory action. Novel compounds with potent MCF-7 cell inhibitory action can be further explored using this QSAR approach.

Acknowledgement: The principal of the VNS Group of Institute Faculty of Pharmacy in Bhopal is acknowledged by the authors for providing the facilities needed to carry out this study.

Conflict of Interest: The authors declare no conflict of interest.

Funding Source: The authors received no financial support for this research.

REFERENCES

1. Giere RN. Science without laws. University of Chicago press; 1999.

2. Perspectives in Biology and Medicine, volume 62, number 4 (autumn 2019): 778-786. https://doi.org/10.1353/pbm.2019.0046 PMid:31761807

3. Nagarajan D, McArdle SE. Immune landscape of breast cancers. Biomedicines. 2018 Feb 11;6(1):20. https://doi.org/10.3390/biomedicines6010020 PMid:29439457 PMCid:PMC5874677

4. Makhoul I, Atiq M, Alwbari A, Kieber-Emmons T. Breast cancer immunotherapy: an update. Breast cancer: basic and clinical research. 2018 May 30;12:1178223418774802. https://doi.org/10.1177/1178223418774802 PMid:29899661 PMCid:PMC5985550

5. Liedtke C, Mazouni C, Hess KR, André F, Tordai A, Mejia JA, Symmans WF, Gonzalez-Angulo AM, Hennessy B, Green M, Cristofanilli M. Response to neoadjuvant therapy and long-term survival in patients with triple-negative breast cancer. Journal of clinical oncology. 2008 Mar 10;26(8):1275-81. https://doi.org/10.1200/JCO.2007.14.4147 PMid:18250347

6. Lehmann BD, Bauer JA, Chen X, Sanders ME, Chakravarthy AB, Shyr Y, Pietenpol JA. Identification of human triple-negative breast cancer subtypes and preclinical models for selection of targeted therapies. The Journal of clinical investigation. 2011 Jul 1;121(7):2750-67. https://doi.org/10.1172/JCI45014 PMid:21633166 PMCid:PMC3127435

7. Landskron G, De la Fuente M, Thuwajit P, Thuwajit C, Hermoso MA. Chronic inflammation and cytokines in the tumor microenvironment. Journal of immunology research. 2014;2014(1):149185. https://doi.org/10.1155/2014/149185 PMid:24901008 PMCid:PMC4036716

8. Barzaman K, Karami J, Zarei Z, Hosseinzadeh A, Kazemi MH, Moradi-Kalbolandi S, Safari E, Farahmand L. Breast cancer: Biology, biomarkers, and treatments. International immunopharmacology. 2020 Jul 1;84:106535 https://doi.org/10.1016/j.intimp.2020.106535 PMid:32361569

9. Erlay J. GLOBOCAN 2012 v1. 0, cancer incidence and mortality worldwide: IARC CancerBase No. 11 (Internet). Int Agency Res Cancer. 2013;42:124.

10. Youlden DR, Cramb SM, Yip CH, Baade PD. Incidence and mortality of female breast cancer in the Asia-Pacific region. Cancer biology & medicine. 2014 Jun 1;11(2):101-15.

11. Housman G, Byler S, Heerboth S, Lapinska K, Longacre M, Snyder N, Sarkar S. Drug resistance in cancer: an overview. Cancers. 2014 Sep 5;6(3):1769-92. https://doi.org/10.3390/cancers6031769 PMid:25198391 PMCid:PMC4190567

12. Jorgensen WL. The many roles of computation in drug discovery. Science. 2004 Mar 19;303(5665):1813-8. https://doi.org/10.1126/science.1096361 PMid:15031495

13. Márquez Martín A, De La Puerta Vázquez R, Fernández-Arche A, Ruiz-Gutiérrez V. Supressive effect of maslinic acid from pomace olive oil on oxidative stress and cytokine production in stimulated murine macrophages. Free radical research. 2006 Jan 1;40(3):295-302. https://doi.org/10.1080/10715760500467935 PMid:16484046

14. Kapoor S. Maslinic acid and its in vitro antineoplastic effects. Nat Prod Res. 2013;27(23):2210-2211. https://doi.org/10.1080/14786419.2013.819506 PMid:24004213

15. Verma J, Khedkar VM, Coutinho EC. 3D-QSAR in drug design-a review. Current topics in medicinal chemistry. 2010 Jan 1;10(1):95-115. https://doi.org/10.2174/156802610790232260 PMid:19929826

16. Cherkasov A, Muratov EN, Fourches D, Varnek A, Baskin II, Cronin M, Dearden J, Gramatica P, Martin YC, Todeschini R, Consonni V. QSAR modeling: where have you been? Where are you going to?. Journal of medicinal chemistry. 2014 Jun 26;57(12):4977-5010. https://doi.org/10.1021/jm4004285 PMid:24351051 PMCid:PMC4074254

17. Ling J, Kumar R. Crosstalk between NFkB and glucocorticoid signaling: a potential target of breast cancer therapy. Cancer letters. 2012 Sep 28;322(2):119-26. https://doi.org/10.1016/j.canlet.2012.02.033 PMid:22433713

18. Alam S, Khan F. 3D-QSAR studies on Maslinic acid analogs for Anticancer activity against Breast Cancer cell line MCF-7. Scientific reports. 2017 Jul 20;7(1):6019. https://doi.org/10.1038/s41598-017-06131-0 PMid:28729623 PMCid:PMC5519539

19. Fuentes N, Silveyra P. Estrogen receptor signaling mechanisms. Adv Protein Chem Struct Biol. 2019;116:135-170. https://doi.org/10.1016/bs.apcsb.2019.01.001 PMid:31036290 PMCid:PMC6533072

20. Hewitt SC, Korach KS. Estrogen receptors: new directions in the new millennium. Endocr Rev. 2018. https://doi.org/10.1210/er.2018-00087 PMid:29901737 PMCid:PMC6173474

21. Folkerd EJ, Dowsett M. Influence of sex hormones on cancer progression. J Clin Oncol. 2010;28:4038-4044. https://doi.org/10.1200/JCO.2009.27.4290 PMid:20644089

22. Zheng B, Zhu Y, Wang HY, Chen L. Gender disparity in hepatocellular carcinoma (HCC): multiple underlying mechanisms. Sci China Life Sci. 2017;60:575-584. https://doi.org/10.1007/s11427-016-9043-9 PMid:28547581

23. Wang LNG, Qian Y, Yang Q, Tan H, Drummer C, Sun Y, et al. A comprehensive data mining study shows that most nuclear receptors act as newly proposed homeostasis-associated molecular pattern receptors. J Hematol Oncol. 2017;10:168. https://doi.org/10.1186/s13045-017-0526-8 PMid:29065888 PMCid:PMC5655880

24. Chen P, Li B, Ou-Yang L. Role of estrogen receptors in health and disease. Front Endocrinol (Lausanne). 2022;13. https://doi.org/10.3389/fendo.2022.839005 PMid:36060947 PMCid:PMC9433670

25. Tang ZR, Zhang R, Lian ZX, Deng SL, Yu K. Estrogen receptor expression and function in female reproductive disease. Cells. 2019;8:1123-1138. https://doi.org/10.3390/cells8101123 PMid:31546660 PMCid:PMC6830311

26. Eyster KM. The estrogen receptors: an overview from different perspectives. Methods Mol Biol. 2016;1366. https://doi.org/10.1007/978-1-4939-3127-9

27. Huang B, Omoto Y, Iwase H, Yamashita H, Toyama T, Coombes RC, et al. Differential expression of estrogen receptor α, β1 and β2 in lobular and ductal breast cancer. Proc Natl Acad Sci U S A. 2014;111:1933-1938. https://doi.org/10.1073/pnas.1323719111 PMid:24449868 PMCid:PMC3918808

28. Johnston SR, Dowsett M. Aromatase inhibitors for breast cancer: lessons from the laboratory. Nat Rev Cancer. 2003;3:821-831. https://doi.org/10.1038/nrc1211 PMid:14668813

29. Anderson WF, Chatterjee N, Brawley OW, Ershler WB. Estrogen receptor breast cancer phenotypes in the surveillance, epidemiology, and end results database. Breast Cancer Res Treat. 2002;76:27-36. https://doi.org/10.1023/A:1020299707510 PMid:12408373

30. Shtaiwi A, et al. Computational investigations of the binding mechanism of novel benzophenone imine inhibitors for the treatment of breast cancer. RSC Adv. 2019;9:35401-35416. https://doi.org/10.1039/C9RA04759J PMid:35541022 PMCid:PMC9082406

31. Lykkesfeldt AE, Sørensen EO. Effect of estrogen and antiestrogens on cell proliferation and synthesis of secreted proteins in the human breast cancer cell line MCF-7 and a tamoxifen-resistant variant subline AL-1. Acta Oncol. 1992;31:131-138. https://doi.org/10.3109/02841869209088892 PMid:1622627

32. Couse JF, Korach KS. Estrogen receptor null mice: what have we learned and where will they lead us? Endocr Rev. 1999;20:358-417. https://doi.org/10.1210/edrv.20.3.0370 PMid:10368776

33. Treeck OJ, Brucker I, Lattrich C, Horn F, Goerse R, Ortmann O, et al. Effects of exon-deleted estrogen receptor β transcript variants on growth, apoptosis and gene expression of human breast cancer cell lines. Breast Cancer Res Treat. 2008;110:507-520. https://doi.org/10.1007/s10549-007-9749-7 PMid:17876701

34. Cotrim CFV, Doria ML, Lindberg K, Gustafsson JÅ, Amado F, et al. Estrogen receptor beta growth inhibitory effects are repressed through activation of MAPK and PI3K signalling in mammary epithelial and breast cancer cells. Oncogene. 2013;32:2390-2402. https://doi.org/10.1038/onc.2012.261 PMid:22751110

35. Speirs V, Malone C, Walton DS, Kerin MJ, Atkin SL. Increased expression of estrogen receptor β mRNA in tamoxifen-resistant breast cancer patients. Cancer Res. 1999;59:5421-5424.

36. Markey GC, Roche PC, Diggin P, Hill AD, McDermott EW, O'Higgins NJ, et al. Estrogen receptor-β mRNA is associated with adverse outcome in patients with breast cancer. Tumor Biol. 2009;30:171-175. https://doi.org/10.1159/000236409 PMid:19738412

37. Marengo SR, Chung LW. An orthotopic model for the study of growth factors in the ventral prostate of the rat: effects of epidermal growth factor and basic fibroblast growth factor. J Androl. 1994;15:277-286. https://doi.org/10.1002/j.1939-4640.1994.tb00450.x

38. Bonkhoff H. Estrogen receptor signaling in prostate cancer: implications for carcinogenesis and tumor progression. Prostate. 2018;78:2-10. https://doi.org/10.1002/pros.23446 PMid:29094395

39. Iyer JK, McCabe KM, Kaul A, Payton ME, Kaul R. Estrogen receptor expression in chronic hepatitis C and hepatocellular carcinoma pathogenesis. World J Gastroenterol. 2017;23:6802-6816. https://doi.org/10.3748/wjg.v23.i37.6802 PMid:29085224 PMCid:PMC5645614

40. Hou JX, Jiang R, Wang Y, Chen C, Deng L, et al. Estrogen-sensitive PTPRO expression represses hepatocellular carcinoma progression by control of STAT3. Hepatology. 2013;57:678-685. https://doi.org/10.1002/hep.25980 PMid:22821478

41. Chen JJ, Tang Y, Huang SF, Ai JG, Wang HX, Zhang LP. HBx protein-induced upregulation of microRNA-221 promotes aberrant proliferation in HBV-related hepatocellular carcinoma by targeting estrogen receptor-α. Oncol Rep. 2015;33:792-798. https://doi.org/10.3892/or.2014.3647 PMid:25483016

42. Yang WL, Yang Y, Xu L, Zheng W, Wu Y, et al. Estrogen represses hepatocellular carcinoma growth via inhibiting alternative activation of tumor-associated macrophages. J Biol Chem. 2012;287:40140-40149. https://doi.org/10.1074/jbc.M112.348763 PMid:22908233 PMCid:PMC3504728

43. Lin VB, Yeh YL, Tu CC, Ho TJ, Lai TY, et al. Activation of estrogen receptors with E2 downregulates peroxisome proliferator-activated receptor-γ in hepatocellular carcinoma. Oncol Rep. 2013;30:3027-3031. https://doi.org/10.3892/or.2013.2793 PMid:24126791

44. Arora P, Arora V, Lamba H, Wadhwa D. Importance of heterocyclic chemistry: a review. Int J Pharm Sci Res. 2012;3:2947-2954.

45. Zadsirjan MM, Vessally H. Prescribed drugs containing nitrogen heterocycles. RSC Adv. 2020;10:44247-44311. https://doi.org/10.1039/D0RA09198G PMid:35557843 PMCid:PMC9092475

46. Hernani PMTF, Silva AL. Synthesis of 2,3,5-substituted pyrrole derivatives. Tetrahedron Lett. 2002;43:4491-4493. https://doi.org/10.1016/S0040-4039(02)00810-9

47. Daidone G, Bivona M, Schillari D. Salicylanilide and its heterocyclic analogs: a comparative study of their antimicrobial activity. Pharmazie. 1990;45:441-442.

48. Almerico AM, Diana P, Barraja P, Dattolo G, Mingoia F, Loi AG, et al. Glycosidopyrroles. Part 3: Effect of benzocondensation on acyclic derivatives: 1-(2-hydroxyethoxy)methylindoles as potential antiviral agents. Il Farmaco. 1998;53:33-40. https://doi.org/10.1016/S0014-827X(97)00002-5 PMid:9543724

49. Schaefer EJ, McNamara JR, Tayler T, Daly JA, Gleason JL, Seman LJ, et al. Comparisons of effects of statins (atorvastatin, fluvastatin, lovastatin, pravastatin, and simvastatin) on fasting and postprandial lipoproteins in patients with coronary heart disease versus control subjects. Am J Cardiol. 2004;93:31-39. https://doi.org/10.1016/j.amjcard.2003.09.008 PMid:14697462

50. Yang D, Bao A, Wei W, Tian L, Huang B, Wang H. Copper-catalyzed domino synthesis of nitrogen heterocycle-fused benzoimidazole and 1,2,4-benzothiadiazine 1,1-dioxide derivatives. ACS Comb Sci. 2015;17:113-119. https://doi.org/10.1021/co500125n PMid:25549532

51. Wermuth CG. The Practice of Medicinal Chemistry. Amsterdam: Elsevier; 2004.

52. Newman DJ, Cragg GM, Snader KM. Natural products as sources of new drugs over the period 1981-2002. J Nat Prod. 2003;66:1022-1037. https://doi.org/10.1021/np030096l PMid:12880330

53. Cragg GM, Newman DJ, Snader KM. Natural products in drug discovery and development. J Nat Prod. 1997;60:52-60. https://doi.org/10.1021/np9604893 PMid:9014353

54. Nepali K, Sharma S, Sharma M, Bedi PM, Dhar KL. Rational approaches, design strategies, structure-activity relationship and mechanistic insights for anticancer hybrids. Eur J Med Chem. 2014;77:422-487. https://doi.org/10.1016/j.ejmech.2014.03.018 PMid:24685980

55. Sandhu S, Bansal Y, Silakari O, Bansal G. Coumarin hybrids as novel therapeutic agents. Bioorg Med Chem. 2014;22:3806-3814. https://doi.org/10.1016/j.bmc.2014.05.032 PMid:24934993

56. Basanagouda M, Veeresh B, Barigidad N, Laxmeshwar S, Devaru S, Venkatesh N. Synthesis and structure-activity relationship of iodinated 4-aryloxymethylcoumarins as potential anticancer and antimycobacterial agents. Eur J Med Chem. 2014;74:225-233. https://doi.org/10.1016/j.ejmech.2013.12.061 PMid:24463645

57. Riveiro ME, Astudillo AM, Vazquez R, Gomez N, Facorro G, Piehl L, et al. Structural insights into hydroxycoumarin-induced apoptosis in U-937 cells. Bioorg Med Chem. 2008;16:2665-2675. https://doi.org/10.1016/j.bmc.2007.11.038 PMid:18060791

58. Erlanson DA, McDowell RS, O'Brien T. Fragment-based drug discovery. J Med Chem. 2004;47:3463-3482. https://doi.org/10.1021/jm040031v PMid:15214773

59. Sun YZ, Fura A, Zhu M, Hanson RL, Roongta V, Humphreys WG. Discovering drugs through biological transformation: role of pharmacologically active metabolites in drug discovery. J Med Chem. 2004;47:4339-4351. https://doi.org/10.1021/jm040066v PMid:15317447

60. Lima LM, Barreiro EJ. Bioisosterism: a useful strategy for molecular modification and drug design. Curr Med Chem. 2005;12:23-49. https://doi.org/10.2174/0929867053363540 PMid:15638729

61. Wermuth CG. Selective optimization of side activities: another way for drug discovery. J Med Chem. 2004;47:1303-1314. https://doi.org/10.1021/jm030480f PMid:14998318

62. Chin CM, Ferreira EI. O processo de latenciação no planejamento de fármacos. Quim Nova. 1999;22:75-81. https://doi.org/10.1590/S0100-40421999000100014

63. Kolb HC, Finn MG, Sharpless KB. Click chemistry: diverse chemical function from a few good reactions. Angew Chem Int Ed. 2001;40:2004-2021. https://doi.org/10.1002/1521-3773(20010601)40:11<2004::AID-ANIE2004>3.0.CO;2-5 PMid:11433435

64. Agalave SG, Maujan SR, Pore VS. Click chemistry: 1,2,3-triazoles as pharmacophores. Chem Asian J. 2011;6:2696-2718. https://doi.org/10.1002/asia.201100432 PMid:21954075

65. Kushwaha K, Kaushik N, Jain S. Design and synthesis of novel 2H-chromen-2-one derivatives bearing 1,2,3-triazole moiety as lead antimicrobials. Bioorg Med Chem Lett. 2014;24:1795-1801. https://doi.org/10.1016/j.bmcl.2014.02.027 PMid:24594353

66. Behbehani H, Ibrahim HM, Makhseed S, Mahmoud H. Applications of 2-arylhydrazononitriles in synthesis: preparation of new indole containing 1,2,3-triazole, pyrazole and pyrazolo[1,5-a]pyrimidine derivatives and evaluation of their antimicrobial activities. Eur J Med Chem. 2011;46:1813-1820. https://doi.org/10.1016/j.ejmech.2011.02.040 PMid:21397366

67. Majeed R, Saeed P, Chinthakindi PK, Khan I, Dangroo NA, Thota N, et al. Synthesis of 3-O-propargylated betulinic acid and its 1,2,3-triazoles as potential apoptotic agents. Eur J Med Chem. 2013;63:782-792. https://doi.org/10.1016/j.ejmech.2013.03.028 PMid:23584541

68. Elamari H, Sapi J, Chabot GG, Quentin L, Scherman D, Girard C. Synthesis and in vitro evaluation of mono- and bis-1,2,3-triazole derivatives of bis-alkynes as potential anticancer agents. Eur J Med Chem. 2013;60:360-364. https://doi.org/10.1016/j.ejmech.2012.12.025 PMid:23314049

69. Kolb HC, Sharpless KB. The growing impact of click chemistry on drug discovery. Drug Discov Today. 2003;8:1128-1137. https://doi.org/10.1016/S1359-6446(03)02933-7 PMid:14678739

70. Zhang W, Li Z, Zhou M, Wu F, Hou X, Luo H, et al. Synthesis and biological evaluation of 4-(1,2,3-triazol-1-yl)coumarin derivatives as potential antitumor agents. Bioorg Med Chem. 2014;24:799-807. https://doi.org/10.1016/j.bmcl.2013.12.095 PMid:24418772

71. Al-Masoudi NA, Pieroni M, Pannecouque C. Nitroimidazoles. Part 7: Synthesis and anti-HIV activity of new 4-nitroimidazole derivatives. Z Naturforsch B. 2012;67:835-842. https://doi.org/10.5560/znb.2012-0122

72. Al-Soud YA, Al-Masoudi NA, Amajaour HA, De Clercq E. Nitroimidazoles. Part 3: Synthesis and anti-HIV activity of new N-alkyl 4-nitroimidazoles bearing benzothiazole and benzoxazole backbones. Z Naturforsch B. 2007;62:523-528. https://doi.org/10.1515/znb-2007-0406

73. Abuteen A, Dietz FZ, Mohammad I, Smith MB, Zhu Q. Synthesis of a 4-nitroimidazole indocyanine dye conjugate and imaging of tumor hypoxia in BALB/c tumor-bearing female mice. Dyes Pigments. 2015;126:251-260. https://doi.org/10.1016/j.dyepig.2015.12.010

74. Varshney V, Misra N, Shukla PK, Sahu DP. Synthesis of nitroimidazole derived oxazolidinones as antibacterial agents. Eur J Med Chem. 2010;45:661-666. https://doi.org/10.1016/j.ejmech.2009.11.009 PMid:19942324

75. Al-Qawasmeh RA, Hasan M, Nedunuri V, Peralta R, Wright J, Lee Y, et al. Potent antimicrobial activity of 3-(4,5-diaryl-1H-imidazol-2-yl)-1H-indole derivatives against methicillin-resistant Staphylococcus aureus. Bioorg Med Chem Lett. 2010;20:3518-3520. https://doi.org/10.1016/j.bmcl.2010.04.137 PMid:20483613

76. Saber SO, Al-Qawasmeh RA, Abu-Qatouseh L, Shtaiwi A, Khanfar MA, Al-Soud YA. Novel hybrid motifs of 4-nitroimidazole-piperazinyl tagged 1, 2, 3-triazoles: Synthesis, crystal structure, anticancer evaluations, and molecular docking study. Heliyon. 2023; 9 (9). https://doi.org/10.1016/j.heliyon.2023.e19327 PMid:37681149 PMCid:PMC10480608

77. Singh AK, Patel J, Jain N, Singour PK. QSAR studies of 2-phenoxyacetamide analogues, a novel class of potent and selective monoamine oxidase inhibitors. Current Research in Pharmaceutical Sciences. 2017:109-16. https://doi.org/10.24092/CRPS.2017.070402